JOURNAL OF CATALYSIS 126, 643–657 (1990)

# Catalytic Hydrodesulfurization by Molybdenum Nitride

E. J. MARKEL AND J. W. VAN ZEE*

*Department of Chemical Engineering, University of South Carolina, Columbia, South Carolina 29208*

Received October 16, 1989; revised May 22, 1990

High surface area molybdenum nitride (up to 108 $m^2/g$) was synthesized, characterized, and tested for thiophene desulfurization activity. The surface area was found to depend on synthesis temperature profile, mass transfer, and passivation procedure. Passivated and sulfided catalysts retained the bulk structure of face-centered-cubic $Mo_2N$. X-ray diffraction and Raman spectroscopy showed no evidence for $MoO_3$ or $MoS_2$ formation in fresh catalysts or catalysts sulfided at 673 K. Thiophene desulfurization activity was measured over a broad range of $Mo_2N$ surface areas and reactor conditions. Small amounts of tetrahydrothiophene were formed during desulfurization and low-conversion data at 673 K indicate that butane is one of the initial products of the thiophene desulfurization reaction, in addition to butadiene and the butenes. 

## INTRODUCTION

Inorganic chemistry provides an abundant variety of metal compounds amenable to catalytic study, but unsuitable for commercial hydrodesulfurization (HDS) use due to their very low surface areas. Recently, molybdenum nitrides ($Mo_2N$) with surface areas as high as 220 $m^2/g$ have been developed (*1–3*) using topotactic reaction methods. The catalytic properties of the high surface area molybenum nitride have been reported in the areas of ammonia synthesis (*4*), quinoline hydrodenitrogenation (HDN) (*5*), CO hydrogenation (*6*), and ethane hydrogenolysis (*6*). This paper is the first to address the application of high surface area $Mo_2N$ to catalytic HDS.

High surface area $Mo_2N$ may be particularly useful for HDS because it consists entirely of active material in contrast to industrial catalyst which contain only 10 to 15% active material dispersed on a support. That is, industrial catalysts consist of sulfided molybdenum or tungsten mixed with smaller amounts of cobalt or nickel promoters (*7*). Because of the low specific surface area of the active phase, these catalysts are dispersed on a high surface area oxide support which does not participate in the desulfurization reaction. Topotactic $Mo_2N$ has an unusually high surface area and thus does not require a support. Topotactic $Mo_2N$ is also unusual because of its resistance to sintering even at 980 K (*1–5*), so that its high surface area should not deteriorate at industrial temperatures. In addition, the electronic properties, the face-centered-cubic crystal structure, and the porous particle morphology (*1, 3, 10*) of topotactic $Mo_2N$ differ from those of the layered $MoS_2$ or $WS_2$ active phase of commercial catalysts (*8*). These differences may affect the functions of the catalyst and provide additional motivation for the study presented here.

One of the goals of this work was to test the resistance of $Mo_2N$ to sulfiding conditions. Previous workers (*9*) have used thermodynamic calculations to predict that nitrides and carbides should be converted to sulfides under high-temperature sulfiding conditions. Also, a study of liquid phase quinoline HDN over high surface area carbides and nitrides (*5*) showed that $CS_2$ changed the reactivity of $Mo_2N$ so that it was similar to $MoS_2$. The work presented

* To whom correspondence should be addressed.



0021-9517/90 $3.00

here examined the resistance of $Mo_2N$ to the severe sulfiding action of 10% $H_2S$ in hydrogen.

Another goal of this work was to develop syntheses for particulate $Mo_2N$. Previous methods for the synthesis of high surface area $Mo_2N$ produced fine powders. A larger, well-defined particle distribution is required for kinetic work because powders can cause nonreproducible and uneven flow of the fluid reactant through the packed bed of catalyst. Also, powders may cause unacceptably large pressure drops in industrial reactors. For these reasons, this work reports synthesis methods and problems encountered during the synthesis of particulate topotactic $Mo_2N$.

## REVIEW

High surface area $Mo_2N$ is produced in a topotactic reaction between $MoO_3$ and flowing $NH_3$. The reaction is termed topotactic because the product $Mo_2N$ has a well-defined crystallographic orientation relative to the $MoO_3$ reactant. Topotactic reaction and the resultant high surface areas are achieved only when the reaction takes place at a slow, controlled rate so that oxygen is removed and replaced with nitrogen without substantial reorganization of the metal lattice. The resulting product is a porous single crystal of $Mo_2N$, pseudomorphous with the parent $MoO_3$, and with $\{100\}_{Mo_2N}$ planes parallel to the original $\{010\}_{MoO_3}$ planes (*1*). The generation of surface area is believed to result when metal reduction begins preferentially at very small linear domains parallel to $\{120\}_{MoO_3}$ planes (*1, 11, 12*). As reduction proceeds in these zones, the metal lattice contracts and fractures the crystal to produce pores.

The preferential reduction of $MoO_3$ along {120} planes may be related to the presence or formation of {120} shear planes such as those common to a number of partially reduced molybdenum oxides (*12, 13*). The shear planes are crystallographic defects created by the aggregation of oxygen vacancies to form planes of molybdenum bound to a tetrahedron of oxygen atoms instead of the octahedrally bound molybdenum of bulk $MoO_3$. The shear planes possess unique structural and chemical properties which may be responsible for the preferential reduction of $MoO_3$ along these planes during temperature-programmed reaction with $NH_3$. In addition, migration of the shear planes may be instrumental in the mechanism for removing oxygen from within the bulk without disturbing the metal lattice.

## EXPERIMENTAL

*Catalyst synthesis.* Procedures for the synthesis of $\gamma$-$Mo_2N$ (fcc) were adapted from the methods of Volpe and Boudart (*1*). Various syntheses were used to produce a range of surface areas. In most cases, $MoO_3$ starting material (Aesar, 3.6 $m^2/g$, 99.995%) was pressed into pellets, lightly crushed, and sieved to produce 40/100 mesh particles. Then, the $MoO_3$ particles were either (a) packed in a 1/8-in.-i.d. fused silica tube between pads of quartz wool or (b) placed in a 1 × 6-in. fused silica boat inside a 2-in.-diameter fused silica tube. The loaded reactors were placed inside a tube furnace and connected to a gas feed system. Flowing ammonia (Matheson, 99.9999%, 3.3 ml(STP)/s) was introduced and the temperature program was initiated, beginning at room temperature and using the heating rates listed in Table 1. The final reaction temperature of 980 K was maintained for 2 h. At the end of the reaction period, the reactors were removed from the furnace with ammonia still flowing (in order to purge the reactor so that air could not enter) and cooled to room temperature. The flow of ammonia was then stopped and air was allowed to contact the sample through 6 ft of $\frac{1}{4}$-in.-i.d. tubing for 12 to 48 h. The sample was considered to be passivated if it did not react when exposed to air to form a light-yellow residue.

As a basis for comparison, industrial-type supported cobalt molybdate catalysts were produced by the pore volume filling method using $\gamma$-$Al_2O_3$ (Norton, 180 $m^2/g$, 40/100

mesh) and aqueous solutions of cobalt nitrate and ammonium molybdate. Loadings of 3 wt% cobalt and 10 wt% molybdenum were selected. After vacuum drying at 393 K, the catalysts were calcined at 673 K in flowing oxygen and then sulfided at 673 K in a mixture of 10% hydrogen sulfide in hydrogen.

*Kinetic measurements.* Thiophene desulfurization rates were measured in a continuous flow, fixed bed reactor. The reactor was constructed of 1/8-in.-i.d. fused silica tubing and contained a bed of 0.100 g catalyst supported between pads of glass wool. A stream of 2.7% thiophene in hydrogen (0.5 ml/s) flowed over the bed of catalyst particles with a superficial space velocity of 10.5 $s^{-1}$. Products were identified by GC–MS and quantified by gas chromatography (FID). Data were stored and integrated by an IBM PC-AT computer using an A/D converter and software produced by Interactive Microware. Each experimental run was begun by heating the catalyst from room temperature to 673 K in the thiophene/hydrogen mixture at 0.125 K/s followed by a catalyst pretreatment step in which 10% hydrogen sulfide in hydrogen flowed over the catalyst at 673 K for 4 h. Reactor feed was then switched to the thiophene/hydrogen mixture and, after a 20-min stabilization period, the analytical system analyzed reaction products every 20 min for a 24-h period.

*Characterization.* Catalysts were characterized both before and after thiophene reaction using X-ray diffraction, Raman spectroscopy, and BET surface area measurements. The fresh, unused catalysts were passivated and exposed to air before analysis; "used" catalysts were sulfided 4 h in 10% $H_2S$ in hydrogen at 400°C, then tested for thiophene desulfurization activity for 24 h and exposed to air before analysis. Catalyst characterization was used to evaluate different preparation procedures and to test the resistance of the $Mo_2N$ structure to sulfiding in the catalytic reactor.

*X-ray diffraction.* Samples were prepared for analysis by grinding with an agate mortar and pestle and then mounted on glass slides using adhesive tape. A Scintag DMC-105 diffractometer (Cu$K\alpha$ radiation) and Data General computer system were used for data collection and analysis. Scans were collected at 1 degree per minute using a 0.02 degree step size.

*Raman spectroscopy.* A Cary model 82 Raman spectrometer was used to record Raman spectra of the solid catalyst samples. The excitation source was a Spectra-Physics model 171 argon ion laser operating at 514.5 nm and 1.0 W. Scattered light was collected at an angle of 90° from the incident laser beam. Spinning sample pellets were used to avoid sample decomposition in the laser beam. Because only small amounts of sample were available for analysis, pellets composed of only a thin layer of sample over a KBr substrate were prepared. Single scans were collected at 4 $cm^{-1}$ resolution and a 20 $cm^{-1}$/min scan rate.

*Surface area.* BET surface areas were measured using a Micromeritics 2700 dynamic adsorption analyzer. Nitrogen was used as the adsorbate. The mass of each sample tested was adjusted to provide approximately 20 $m^2$ surface area. The standard deviation of the surface area measurements of eight portions of the same catalyst sample was found to be 2.9%. Each sample was tested three times and the average of the three measurements is reported.

## RESULTS

*Catalyst synthesis.* Representative $Mo_2N$ preparations and resultant surface areas are listed in Table 1. As reported previously (*1*), the temperature ramping rate was found to influence surface area. Catalysts B1–B5 were synthesized to study the effect of the temperature ramping rate on surface area. Preparations B1–B3 used temperature ramps of 5 K/min or less and produced catalysts with specific areas of approximately 50 $m^2/g$. Temperature ramps of 10 K/min and 20 K/min resulted in $Mo_2N$ with sharply lower surface areas of 12.9 and 6.0 $m^2/g$, respectively. The possibility of producing

TABLE 1

Synthesis Conditions and Resultant Surface Areas

| Catalyst | Apparatus | Sample size (g) | Heating rate (K/min) | Surface area ($m^2/g$) |
|---|---|---|---|---|
| A1 | a | 1.0 | 0.6 | 42.0 |
| A2 | b | 1.0 | 0.6 | 78.7 |
| A3 | c | 1.0 | 0.6 | 102. |
| A4 | c | 0.1 | 0.6 | 108. |
| B1 | b | 5.0 | 0.6 | 54.2 |
| B2 | b | 5.0 | 2.0 | 48.8 |
| B3 | b | 5.0 | 5.0 | 52.0 |
| B4 | b | 5.0 | 10.0 | 12.9 |
| B5 | b | 5.0 | 20.0 | 6.0 |

*Note.* Apparatus: (a) $MoO_3$, fine powder bed in fused-silica boat; (b) $MoO_3$, 40/100 mesh particles in fused-silica boat; (c) $MoO_3$, 40/100 mesh particles, packed bed in fused-silica tube. In all cases, temperature was ramped from room temperature to a final reaction temperature of 980 K, which was maintained for 2 h.

low surface areas using temperature programs with higher final reaction temperatures was also tested, but these preparations were found to produce $Mo_2N$ containing large amounts of metallic molybdenum and MoN impurities.

Mass transfer-related variables were also found to influence surface areas. For example, catalysts A1–A4 were prepared using identical temperature programs but different particle sizes and packed bed configurations, resulting in surface areas ranging from 42.0 to 108 $m^2/g$. The preparation of catalyst Al (42.0 $m^2/g$) required ammonia to diffuse into a bed of fine $MoO_3$ powder and required reaction products such as $H_2O$ to diffuse out of the powder. The preparation for catalyst A2 improved the gas contacting scheme by enlarging the $MoO_3$ particle size, thus improving the ability of gases to diffuse into and out of the bed of particles and resulting in a higher specific surface area (78.7 $m^2/g$). A comparison of catalysts A2 and B1 also illustrates the effect of diffusion on surface area: preparation B1 produced lower surface areas because gases were required to diffuse through a particle bed approximately five times as thick as that of preparation A2. Catalysts A3 and A4 achieved the highest surface areas of this study using forced convection of ammonia through a packed bed of $MoO_3$ particles. Still higher surface areas would be expected if $Mo_2N$ was synthesized by flow through a packed bed of finer $MoO_3$ powder (*1*). However, as discussed above, the kinetic measurements of this study required the use of larger, well-defined particle sizes. Because the powdered $Mo_2N$ product was not sufficiently cohesive to produce larger particles, suitable particles were made using 40/100 mesh $MoO_3$ reactant to produce 40/100 mesh $Mo_2N$.

Lower surface areas may result when hindered mass transfer either allows the accumulation of $H_2O$ in the bed or limits ammonia/solid contact. The presence of even small amounts of water has been shown to cause hydrothermal sintering (*2, 14*). Catalytic decomposition of $NH_3$ (*1, 2*) may also produce $NH_3$ gradients within beds in which mass transfer is limited. Either effect may interfere with the topotactic reaction mechanism and reduce surface area.

Specific surface area may also be influenced by $NH_3$ space velocity. The effect is observed by comparison of catalysts A3 and A4, whose preparations differ only in sample weight: the smaller sample mass (A4) is

synthesized at a higher space velocity (for constant $NH_3$ flowrate) and produces a catalyst with slightly higher surface area. The smaller space velocity produces higher concentrations of $H_2O$ and larger axial $NH_3$ gradients which both may affect the topotactic reaction mechanism as mentioned previously. Although the effect is small when comparing catalysts A3 and A4 (prepared at very high space velocities), lower space velocities may magnify the effect. Previous workers (*2*) have shown that higher $Mo_2N$ surface areas are produced at higher space velocities. The surface area of sample A3 (102 $m^2/g$, space velocity = 16,000 $h^{-1}$) agrees well with the literature value of surface area produced at 14,000 $h^{-1}$ (88 $m^2/g$). The surface area of catalyst A4 (108 $m^2/g$ at a space velocity of 160,000 $h^{-1}$) is much smaller than the value predicted by the literature (>200 $m^2/g$), probably because limited intraparticle mass transfer is lowering the surface area of the particulate $Mo_2N$ from the value predicted for a fine powder.

The effect of passivation on surface area was not examined here but passivation has been shown to decrease surface area (*1*). All catalyst samples in this work were passivated and then exposed to air. The amount of time required to form a stable (i.e., passivated) sample varied from 12 to 48 h. Incompletely passivated $Mo_2N$ reacted rapidly when exposed to air to form a light-yellow residue which was identified by Raman spectroscopy as $MoO_3$. Generally, higher surface area catalysts required longer passivation periods.

*Characterization, fresh catalysts.* Powder X-ray diffraction was used to analyze fresh catalysts prepared using different temperature programs (Fig. 1). The location of diffraction peaks agreed well with literature values for $\gamma$-$Mo_2N$ (*15*). Diffraction data show no evidence of impurities in the freshly prepared samples with the exception of samples prepared at 10 and 20 K/min heating rates which contain small amounts of MoN ($2\theta$ = 48.8). X-ray diffraction peak intensities for the low surface area samples are

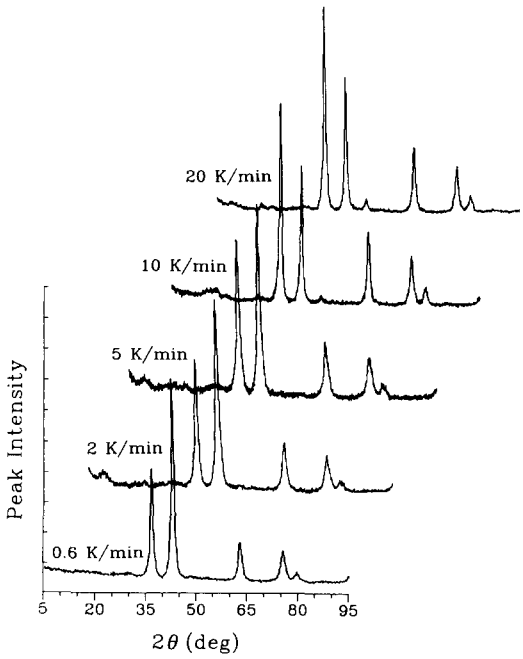


FIG. 1. Powder X-ray diffraction patterns of $Mo_2N$ samples B1–B5, prepared at various temperature ramping rates and passivated by exposure to air.

similar to those reported in the literature (*15*). High surface area $Mo_2N$ produced more intense {200} peaks ($2\theta$ = 43.2) than low surface area $Mo_2N$, as previously reported for topotactic $Mo_2N$ (*3*).

Fresh catalyst particle diameters (Table 2) were estimated from surface area, $S_g$, using $D_p = 6/\rho S_g$ and assuming a density for $Mo_2N$ of 9.5 $g/cm^3$ (*1*). These values represent an average for a distribution of particle sizes and may be influenced by differences in particle morphology. Particle sizes were also calculated from the {111} and {200} X-ray diffraction line widths using the Scherrer equation (*16*),

$$D_p = K\lambda/\beta \cos\theta$$

assuming a value of 1.0 for $K$ and correcting the measured linewidths ($\beta$) for the effects of instrumental broadening. Particle sizes calculated by the two methods (XRD linewidths and surface area) agree quite well for high surface area catalysts B1, B2, and B3.

TABLE 2

Particle Sizes of Fresh Catalysts

| Catalyst | Surface area ($m^2/g$) | Particle size (nm) | | |
|---|---|---|---|---|
| | | From $S_g$[a] | From XRD[b] {111} | From XRD[c] {200} |
| B1 (0.6 K/min) | 54.2 | 11.7 | 12.8 | 14.9 |
| B2 (2.0 K/min) | 48.8 | 12.9 | 11.1 | 11.6 |
| B3 (5.0 K/min) | 52.0 | 12.1 | 11.1 | 11.6 |
| B4 (10.0 K/min) | 12.9 | 49.1 | 17.3 | 17.1 |
| B5 (20.0 K/min) | 6.0 | 106. | 17.0 | 16.7 |

[a] From specific surface area, $D_p = 6/\rho S_g$.
[b] From corrected {111} peak width, Scherrer equation.
[c] From corrected {200} peak width, Scherrer equation.

Agreement is very poor, however, for the low surface area particles and may indicate the low surface area particles are polycrystalline. The topotactic $Mo_2N$ particles are not spherical: the dimensions of the diffracting domains perpendicular to the {200} planes are slightly larger than those perpendicular to the {111} planes. Note that these differences disappear in nontopotactic samples B4 and B5.

The Raman spectrum of fresh $Mo_2N$ (synthesis B1, 54 $m^2/g$) is shown in Fig. 2. The spectrum consists of two broad peaks at 590 and 1100 $cm^{-1}$. Notable is the absence of peaks due to the formation of $MoO_3$ (a strong Raman scatterer with peaks at 818 and 994 $cm^{-1}$). Oxygen incorporated during passivation is not detected as a distinct molybdenum oxide phase except perhaps as an irregular surface phase responsible for the uneven baseline between 700 and 1000 $cm^{-1}$.

*Characterization, sulfided catalysts.* Catalysts were removed from the reactor after use and analyzed by X-ray diffraction and Raman spectroscopy. Diffraction data for catalyst B1 are presented in Fig. 3. Peak locations and relative intensities show that the bulk structure of topotactic $Mo_2N$ was

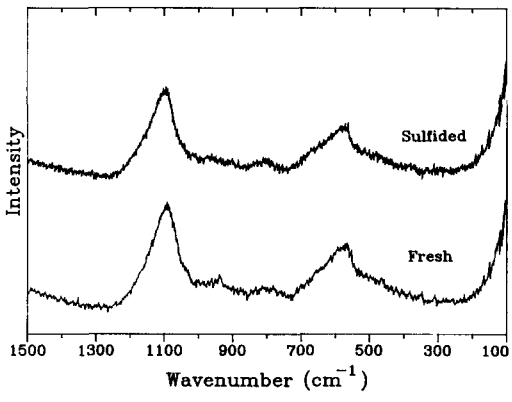


FIG. 2. Raman spectra of fresh and sulfided $Mo_2N$; sample B1.

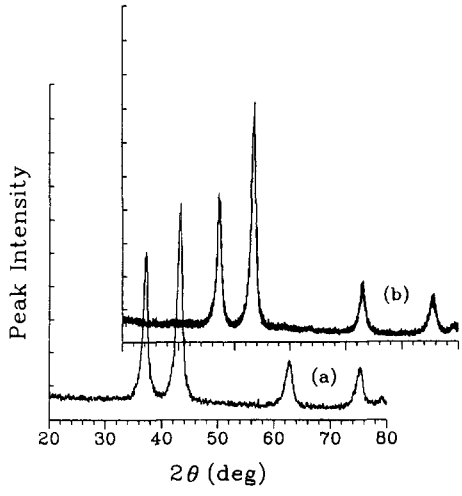


FIG. 3. Powder X-ray diffraction patterns of (a) fresh and (b) sulfided $Mo_2N$; sample B1.

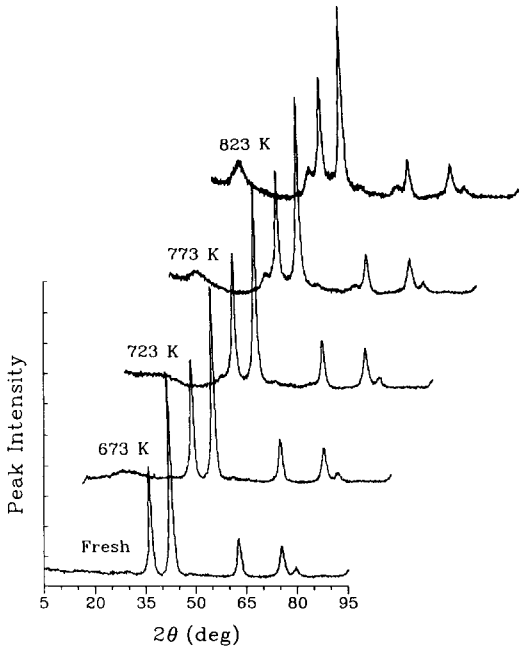


FIG. 4. Powder X-ray diffraction patterns of $Mo_2N$ (catalyst B1) sulfided 4 h in 10% $H_2S$ in hydrogen at elevated temperatures.

retained and no traces of impurities such as $MoS_2$ or $MoO_3$ are found. The Raman spectrum of the sulfided catalyst (Fig. 2) also showed no evidence of impurities; bands at 383 and 409 $cm^{-1}$ due to $MoS_2$ formation are not detected.

The specific surface areas of catalysts removed from the reactor after 24 h of reaction are listed in Table 4. Surface areas were generally found to decrease only slightly as a result of 4 h of sulfiding followed by 24 h of thiophene reaction. Some catalysts showed measured increases in surface area after reaction but the small increases in surface area are smaller than the expected variance in the surface area measurement of ±3%. Sample A3 reacted with air when removed from the reactor while still warm (and hence, no postreaction surface area is reported) but the other sulfided samples were generally much less air-sensitive than fresh $Mo_2N$.

To test the resistance of the $Mo_2N$ catalysts to severe sulfiding conditions, samples (catalyst B1, 54.2 $m^2/g$) were sulfided in the packed bed reactor for 4 h in 10% $H_2S$ in hydrogen at 673, 723, 773, and 823 K. The X-ray diffraction data for these samples (Fig. 4) show the bulk structure of topotactic $Mo_2N$ is retained even for samples sulfided at 823K, although some $MoS_2$ is formed at 773 and 823 K. Surface area and particle size estimates for these samples are summarized in Table 3. Catalyst samples sulfided at 673 K show very little surface area loss upon sulfiding while samples sulfided at higher temperatures experience significant surface area losses. Particle diameters calculated from surface area and X-ray linewidths agree quite well for high surface area samples, but as surface area drops, the particle

TABLE 3

Particle Sizes of Sulfided Catalysts

| Catalyst | Surface area ($m^2/g$) | Particle size (nm) | | |
|---|---|---|---|---|
| | | From $S_g$[a] | From XRD[b] {111} | From XRD[c] {200} |
| Fresh | 54.2 | 11.7 | 12.8 | 14.9 |
| Sulfided, 673 K | 53.1 | 11.9 | 12.7 | 14.9 |
| Sulfided, 723 K | 42.2 | 14.9 | 12.5 | 14.6 |
| Sulfided, 773 K | 35.0 | 18.0 | 12.8 | 13.4 |
| Sulfided, 823 K | 27.1 | 23.3 | 12.2 | 11.9 |

[a] From specific surface area, $D_p = 6/\rho S_g$.
[b] From corrected {111} peak width, Scherrer equation.
[c] From corrected {200} peak width, Scherrer equation.

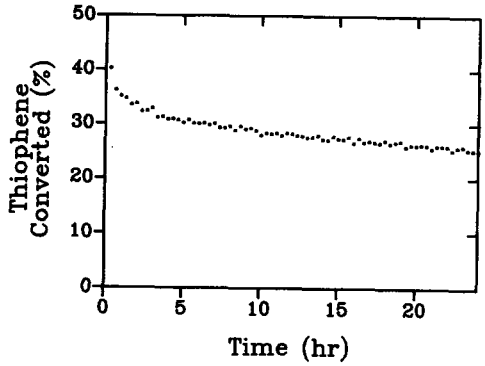


FIG. 5. Catalytic activity at 673 K during 24-h thiophene desulfurization run; catalyst B1.

sizes calculated from diffraction data do not increase. Instead, the dimensions of diffraction domains perpendicular to the {111} plane remain fairly constant while dimensions perpendicular to {200} actually decrease. These data indicate that the surface area change is probably not due to sintering, in which enlarged diffraction domains and narrowed XRD lines are expected. Instead, surface area losses may be due to conversion of $Mo_2N$ to $MoS_2$, resulting in smaller $Mo_2N$ domains and blockage or restriction of small pores in $Mo_2N$ particles by less dense $MoS_2$.

*Catalytic activities.* Each catalyst was tested for thiophene desulfurization activity under identical reaction conditions. Identical catalyst sample weight, thiophene concentration, hydrogen flow rate, temperature program, and pretreatment steps were used as described previously. Catalyst activity throughout a 24-h run is illustrated in Fig. 5.

Thiophene conversions for each catalyst at the end of the 24-h test period are shown in Table 4. To a first approximation, catalyst activity (expressed as percent thiophene conversion) was found to be proportional to catalyst surface area. However, low surface area catalysts B4 and B5 deviated sharply from this trend, exhibiting much higher specific activity than the high surface area catalysts. High surface area catalysts A3 and A4 produced the lowest specific activities while catalyst areas between 40 and 80 $m^2/g$ produced intermediate specific activities.

The thiophene desulfurization activity of a cobalt molybdate supported catalyst was also tested. Thiophene conversion of 49.8% was achieved at the end of a 24-h run using 0.100 g of the reference catalyst. To compare the performance of the cobalt molybdate supported catalyst and $Mo_2N$ catalysts, it is important to note that the bed volume of 0.1 grams of 40/100 mesh $Mo_2N$ was measured to be only 45% as large as the bed

TABLE 4

Thiophene HDS Activity Measured After 24 h of Reaction Under Standardized Conditions, 400°C

| Catalyst | Surface area | | Catalytic activity | |
|---|---|---|---|---|
| | Fresh ($m^2/g$) | Postreaction ($m^2/g$) | Conversion (%) | (mol/$sm^2$) $\times 10^8$ |
| A1 | 42.0 | 45.0 | 17.7 | 2.32 |
| A2 | 78.7 | 69.0 | 32.2 | 2.26 |
| A3 | 102. | — | 35.4 | 1.92 |
| A4 | 108. | 99.8 | 38.1 | 1.95 |
| B1 | 54.2 | 48.3 | 25.2 | 2.56 |
| B3 | 52.0 | 47.2 | 21.1 | 2.23 |
| B4 | 12.9 | 13.0 | 10.5 | 4.49 |
| B5 | 6.0 | 6.2 | 19.4 | 17.84 |

*Note.* Catalyst $A_3$ reacted with air when removed from reactor.

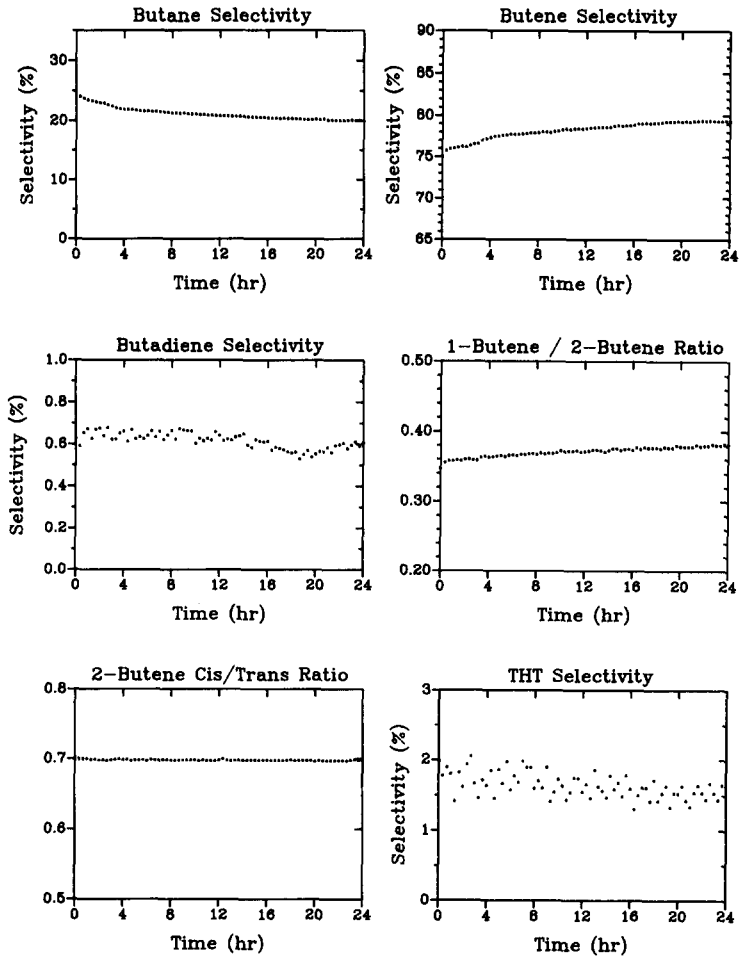


FIG. 6. Product Selectivities at 673 K during 24-h thiophene desulfurization run; catalyst B1.

volume of 0.1 grams of the 40/100 mesh supported cobalt molybdate catalyst. Furthermore, if the void volume is the same for both 40/100 mesh catalyst beds, the residence time in the cobalt molybdate bed was more than twice as large as the residence time in the $Mo_2N$ bed when using equal weights of $Mo_2N$ and cobalt molybdate catalysts.

*Catalyst selectivities.* Butadiene, 1-butene, *cis*-2-butene, *trans*-2-butene, *n*-butane, and hydrogen sulfide were the principal desulfurization products. Small amounts of tetrahydrothiophene were also detected in the reactor effluent. Isobutane and smaller hydrocarbon fragments were detected as well, but this group represented a total of less than 0.5% of the total desulfurization products and were not examined closely.

Product selectivities are expressed as percent of the total amount of desulfurized $C_4$ hydrocarbons and are summarized for a 24-h run employing catalyst B1 in Fig. 6. Butenes were the predominant desulfurization products; *cis*-2-butene and *trans*-2-butene were always produced in a constant 7 : 10 ratio, characteristic of thermodynamic equilibrium of the isomers (*17*), but the 1-butene : 2-butene ratio varied slightly from its equilibrium value of 0.34 (*17*). Butane and butadiene were produced in lesser amounts. Tet-

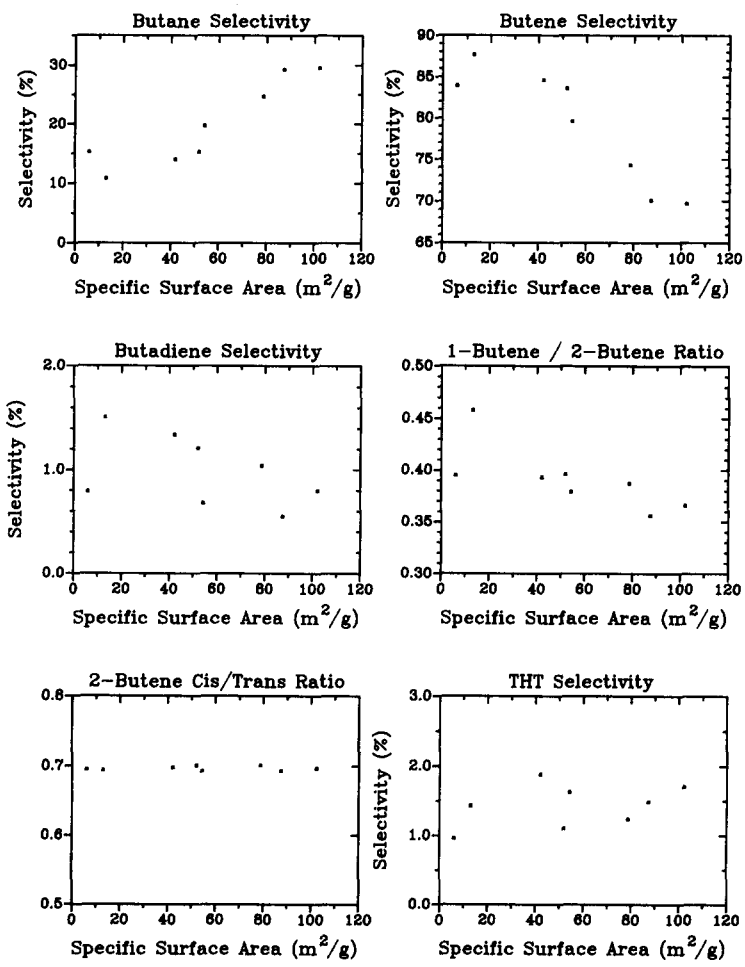


FIG. 7. Product selectivities at 673 K, $Mo_2N$ catalysts A1–A4, B1–B5, measured at end of 24-h thiophene desulfurization period, as a function of catalyst surface area.

rahydrothiophene selectivity is also shown in Fig. 6. The data are scattered, due to the difficulty of integrating the broad tetrahydrothiophene peak located at the end of each chromatogram.

Product selectivities for all catalysts at the end of the 24-h standard reaction period are summarized in Fig. 7. Catalysts are identified in these figures by their surface area. Interestingly, these chemically equivalent catalysts exhibited distinct differences in selectivity which appear to be a function of catalyst surface area. Selectivities were also plotted as a function of thiophene conversion (Fig. 8) and were found to correlate much more closely with conversion than with catalyst suface area.

The selectivity data of Figs 7 and 8 lead to the hypothesis that differences in catalyst selectivity were a function of extent of conversion instead of catalyst surface area or some other physical or chemical property. The initial products of desulfurization ($P'$) may be converted in hydrogenation or isomerization reactions to yield different product distributions ($P''$):

$$\text{Thiophene} \rightarrow \begin{matrix} P_i' \\ P_j' \\ P_k' \end{matrix} \rightarrow \begin{matrix} P_i'' \\ P_j'' \\ P_k''. \end{matrix}$$

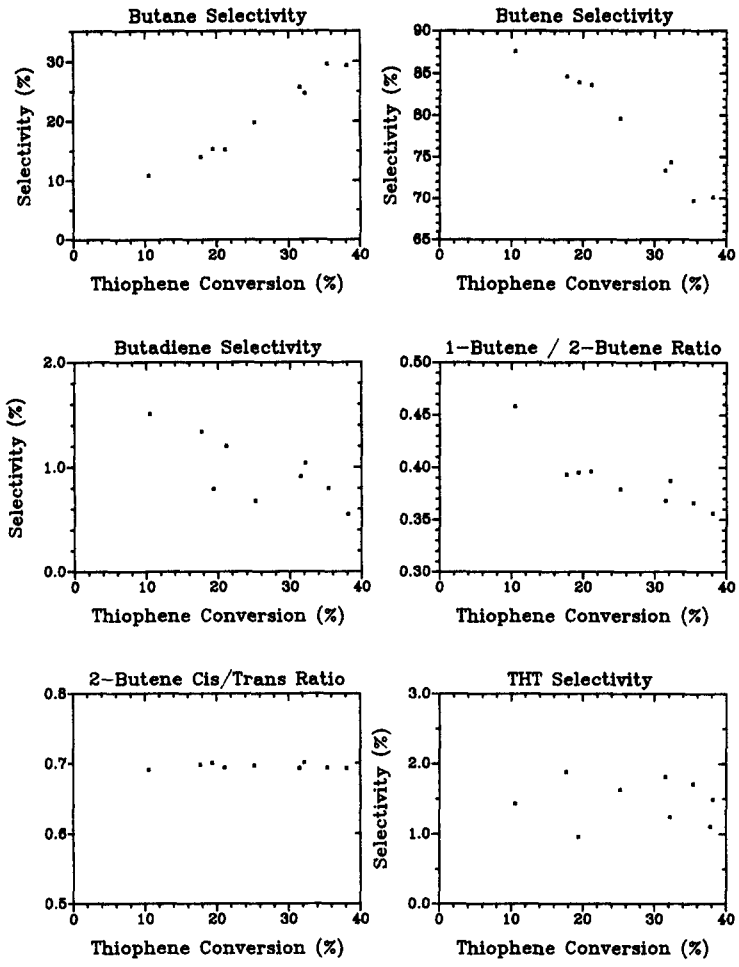


FIG. 8. Product selectivities at 673 K, $Mo_2N$ catalysts A1–A4, B1–B5, measured at end of 24-h thiophene desulfurization period, as a function of thiophene conversion.

The effects of these subsequent reactions are diminished at differential conversion levels so that the initial product distribution ($P'$) is observed. Thus, the different selectivities observed for high and low surface area $Mo_2N$ catalysts may be due to reactions which convert butadiene to butenes, isomerize butenes, or convert butenes to butane.

To test this hypothesis, the reaction conditions were changed to produce lower conversion from high surface area catalysts. This was done by increasing the reactant flow rate (at constant thiophene concentration) from 0.5 ml/s to 1.0, 2.0, and 4.0 ml/s and/or by reducing the mass of $Mo_2N$ catalyst in the packed bed (with the aid of an inert silica diluent). Three catalysts with a broad range of surface areas were chosen for these low conversion experiments. One of these catalysts (B1, 54.2 $m^2/g$) was diluted to approximately 50, 25, and 12 mass percent $Mo_2N$ using $SiO_2$. Packed beds containing 0.100 g of these catalysts (or catalyst–silica mixtures) were heated to 673 K in 2.9% thiophene in hydrogen (0.5 ml/s), then sulfided as before at 673 K, and finally switched back to the thiophene feed mixture for a 24-h reaction period. The analytical system

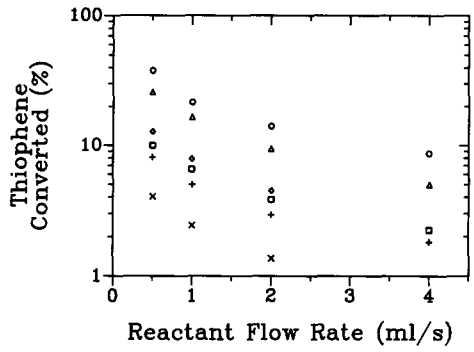


FIG. 9. $Mo_2N$ catalyst activities over a range of reactant space velocities. Symbols correspond to catalysts: (○) A3, (△) B1, (□) B4, (◇) 50% B1 in $SiO_2$, (+) 25% B1, (×) 12% B1.

sampled the reactor effluent every 20 min near the end of the 24-h period to obtain activity and selectivity at the 0.5 ml/s flow rate. At the 24-h mark, the thiophene/hydrogen flow rate was increased to 1.0 ml/s and the gas/liquid feed system was allowed to stabilize for 1 h. Activity and selectivity were measured at the end of the 1 h stabilization period. Similar procedures were used to collect data at 2.0 and 4.0 ml/s, but only 20 min were required for the gas/liquid feed system to stabilize at these rapid flow rates.

As expected, lower thiophene conversions were achieved at increased space velocities (Fig. 9). The lowest thiophene conversions achieved were 2.24% for a pure $Mo_2N$ sample and 1.36% for a diluted $Mo_2N$ sample. Thus, these experiments provide data at conversions ranging from 1.36% to 38.1%.

Product selectivities from the low conversion experiments are summarized in Fig. 10. These plots clearly show that product selectivities are functions of thiophene conversion and are not intrinsic of each particular catalyst. For example, the butane selectivity of catalyst A3 does not remain constant when reactant velocity increases to 4.0 ml/s. Instead, the butane selectivity of catalyst A3 falls from 30 to 11%. Furthermore, Fig. 10 includes selectivity data obtained by permutations of three variables (reactant flow rate, $Mo_2N$ surface area, and mass of $Mo_2N$ in the bed) which, nevertheless, correlate well with percent thiophene conversion.

## DISCUSSION

*Passivated catalyst structure.* Passivated molybdenum nitride catalysts exhibit the bulk structure of face-centered-cubic $\gamma$-$Mo_2N$. Previous workers (*1*) have described the structure of topotactic $Mo_2N$ as a porous crystal. The X-ray diffraction line broadening data of Table 2 support this model: the close agreement of particle sizes calculated from surface area and the dimensions of diffracting crystalline domains indicate a high degree of crystallinity. Nontopotactic catalysts (B4 and B5), on the other hand, consist of somewhat larger crystalline domains which are much too small to be responsible for the low surface area. These samples are polycrystalline.

Oxygen is incorporated into the samples during passivation: elemental analysis has been used (*3*) to estimate the amount of oxygen present in passivated $Mo_2N$ to be as large as 19% of the total amount of nitrogen present in pure $Mo_2N$. Theoretical monolayer oxidation of the 3.4-nm particles used in that study (assuming that oxygen displaces nitrogen in the metal lattice at the surface) would result in replacement of 17% of lattice nitrogen with oxygen. However, X-ray diffraction data (Figs. 1, 3, 4) show no evidence of crystalline molybdenum oxide formation and only very weak and broad Raman peaks (Fig. 2) suggest the presence of molybdenum–oxygen bonds. Therefore, we conclude that passivation produces a protective, amorphous, surface oxide slightly greater than one-monolayer thick.

*Sulfided catalyst structure.* Sulfided catalysts have essentially the same Raman spectrum and XRD pattern as fresh catalysts. $MoS_2$ and $MoO_3$ are not observed. It is possible to produce observable amounts of $MoS_2$ under extreme sulfiding conditions. These severely sulfided samples lose surface area by the clogging and restriction of

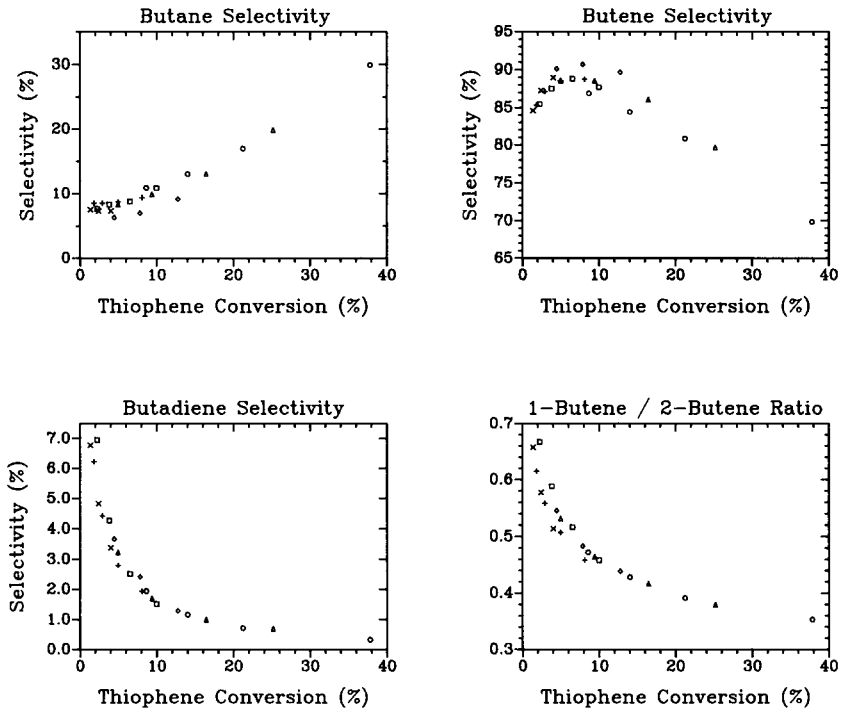


FIG. 10. Product selectivities over a range of reactant space velocities, low conversion experiments. For reasons of clarity, space velocities are not indicated explicitly, but may be deduced from thiophene conversion using Fig. 9.

pores by $MoS_2$ (which is less dense than $Mo_2N$). Surface area loss under the severe sulfiding conditions is not due to sintering: $Mo_2N$ particles actually become smaller as molybdenum is consumed to form $MoS_2$. XRD data show that molybdenum is consumed preferentially from {200} faces of particles during the sulfiding of $Mo_2N$.

The surface structure of the sulfided $Mo_2N$ catalysts cannot be determined from the available structural data. However, the relatively high selectivity of sulfided $Mo_2N$ for tetrahydrothiophene and butane is not observed from unsupported $MoS_2$ (*18*) and supported molybdate catalysts (*19*) tested under similar conditions. The surface structure of sulfided $Mo_2N$, therefore, differs from that of $MoS_2$ and supported molybdate catalysts.

*Catalyst activities*. Specific catalyst activities are similar to those reported for other unsupported molybdenum catalysts tested under similar conditions (see Table 5). The $Mo_2N$ catalysts, of course, are much more active on a weight basis due to their much higher specific surface areas. Low surface area $Mo_2N$ was found to have much higher activities *per square meter* than the higher surface area catalysts. Although catalyst activities have been reported to be sensitive to particle size for supported iron particles in the range below 5 nm in diameter (*20, 21*), the present particles fall outside this range of sensitivity and particle size is not expected to influence specific catalyst activity. The high specific activities at low surface area are possibly due to the presence of small amounts of MoN which were detected by X-ray diffraction in both catalyst B4 and B5. The MoN component may be much more active than $Mo_2N$: studies of unsupported molybdenum Chevrel phase catalysts have shown the importance of molybdenum in oxidation states between two and

TABLE 5

Thiophene HDS Rate, Literature Values (Ref (*18*))

| Catalyst | Surface area ($m^2/g$) | Thiophene conversion (%) | HDS rate ($mol/sm^2$) $\times 10^8$ |
|---|---|---|---|
| $MoS_2$ | 3.4 | 0.76 | 0.92 |
| $Co_{0.25}MoS$ | 10.83 | 0.77 | 2.92 |
| $Co_{1.5}Mo_6S_8$ | 0.15 | 0.54 | 0.82 |
| $AgMo_6S_8$ | 0.438 | 1.19 | 2.34 |
| $HoMo_6S_8$ | 0.579 | 2.20 | 11.23 |

four (*18, 22*). The formal oxidation state of molybdenum in MoN is three. A $Mo^{3+}$ ESR signal from supported molybdate catalysts has been correlated with thiophene desulfurization activity (*23*).

*Catalyst selectivities.* The observed distributions of $C_4$ hydrocarbon products were found to be affected by hydrogenation and isomerization side reactions. The identification of the products of thiophene desulfurization can only be made at low conversions where the effects of side reactions are diminished. Selectivity data indicate an increase in butadiene formation at low conversions. Many proposed pathways for thiophene hydrodesulfurization include butadiene as an initial product of thiophene desulfurization, but recognize that butadiene is rapidly hydrogenated to form butenes and butane. Such a model is consistent with the present butadiene selectivity data, but the low levels of butadiene detected would not support the role of butadiene as the predominant product of desulfurization. Selectivity data at even lower extents of conversion are required to ascertain the predominance of a desulfurization route in which butadiene is formed.

The profile for butene selectivity is typical for an intermediate in a series of chemical reactions: selectivity first rises and then falls with extent of reaction. This profile, however, does not establish butadiene as the sole initial product of desulfurization. In fact, it is possible that significant amounts of butenes are produced directly as products of desulfurization and the observed rise in butene selectivity at low conversions is only a small addition of butene produced by butadiene hydrogenation. The distribution of the butenes indicate a slight preference for 1-butene formation at low conversions. This result has been observed many times previously (*7, 18, 19*) and is consistent with a model in which butadiene is hydrogenated to form predominantly 1-butene which may be subsequently isomerized to produce a thermodynamic equilibrium of butene isomers.

The butane selectivity data at low conversion is particularly interesting because the data do not approach the *y*-axis asymptotically. It is possible to extrapolate the low conversion butane selectivity data to obtain a value for butane selectivity at differential conversion between 6 and 8%. Butane is, therefore, observed as one of the direct products of thiophene hydrodesulfurization, although only 6 to 8% of desulfurized thiophene follows this route. Given the observations of butadiene and butane as direct products of desulfurization, it is very likely that the butenes (the most predominant products observed) are also direct products of desulfurization.

## SUMMARY

High surface area $Mo_2N$ is stable at 673 K under sulfiding (10% $H_2S/H_2$) and thiophene reaction conditions. The high surface area samples were found to consist of small single crystals of pure $Mo_2N$ while the low sur-

face area samples were polycrystalline and contained small amounts of MoN. No evidence was found for the formation of bulk molybdenum oxides or oxynitrides in passivated $Mo_2N$ samples.

Specific thiophene desulfurization rates were found to be similar to those of unsupported catalysts with much lower surface areas. Analysis of the product distributions showed that thiophene desulfurizes over $Mo_2N$ to directly form butadiene, butane, and the butenes. Butadiene is rapidly consumed in hydrogenation reactions to form butenes; at larger extents of reaction, the butenes are consumed to form the most thermodynamically stable product, butane. These product distributions indicate that $Mo_2N$ catalysts are much stronger hydrogenation catalysts than the supported cobalt-molybdate catalyst. Thus, even though high hydrogenation activity may not be a desirable property for an HDS catalyst due to the expense of hydrogen feedstocks, topotactic $Mo_2N$ provides a basis for a new class of promoted catalyst systems. These new catalysts have considerable potential due to the stability of $Mo_2N$ under sulfiding conditions and the very high HDS activity reported herein.

## ACKNOWLEDGMENTS

This work was supported by an unrestricted grant from the DuPont Company, and by the College of Engineering and the Department of Chemical Engineering at the University of South Carolina.

## REFERENCES

1. Volpe, L., and Boudart, M., *J. Solid State Chem.* **59,** 332 (1985).
2. Oyama, S. T., Schlatter, J. C., Metcalf, J. E., and Lamberg, J. M., *Ind. Eng. Chem. Res.* **27,** 1639 (1988).
3. Ranhotra, G. S., Haddix, G. W., Bell, A. T., and Reimer, J. A., *J. Catal.* **108,** 24 (1987).
4. Volpe, L., and Boudart, M., *J. Phys. Chem.* **90,** 4878 (1986).
5. Schlatter, J. C., Oyama, S. T., Metcalf, J. E., and Lambert, J. M., *Ind. Eng. Chem. Res.* **27,** 1648 (1988).
6. Ranhotra, G. S., Bell, A. T., and Reimer, J. A., *J. Catal.* **108,** 40 (1987).
7. Massoth, F. E., and MuraliDhar, G., *in* "Proceeding of the Climax Fourth International Conference on the Chemistry and Uses of Molybdenum" (H. F. Barry and P. Mitchell, Eds.), p. 343. Climax Molybdenum, Ann Arbor, MI, 1982.
8. Topsoe, H., and Clausen, B. S., *Catal. Rev. Sci. Eng.* **26,** 395 (1984).
9. Levy, R. B., *in* "Advanced Materials in Catalysis" (J. J. Burton and R. L. Garten, Eds.), p. 101. Academic Press, San Diego, 1977.
10. Lee, J. S., Volpe, L., Ribiero, F. H., and Boudart, M., *J. Catal.* **112,** 44 (1988).
11. Koenig, H., *Z. Phys.* **130,** 483 (1951).
12. Bursill, L. A., *Proc. Roy. Soc. A* **311,** 267 (1969).
13. Magneli, A., *Acta Cryst.* **6,** 495 (1953).
14. Horlock, R. F., Morgan, P. L., and Anderson, P. J., *Trans. Faraday Soc.* **59,** 721 (1963).
15. Berry, L. G., Ed., JCPDS Powder Diffraction File (Inorganic), 1971.
16. Klug, H. P., and Alexander, L. E., *in* "X-Ray Diffraction Procedures," p. 511. Wiley, New York, 1963.
17. Benson, S. W., and Bose, A. W., *J. Amer. Chem. Soc.* **85,** 1385 (1963).
18. McCarty, K. F., Anderegg, J. W., and Schrader, G. L., *J. Catal.* **93,** 375 (1985).
19. Markel, E. J., Schrader, G. L., Sauer, N. N., and Angelici, R. J., *J. Catal.* **116,** 11 (1989).
20. Dumesic, J. A., Topsoe, H., and Boudart, M., *J. Catal.* **37,** 513 (1975).
21. Boudart, M., *in* "Proceeding, Sixth International Congress on Catalysis, London, 1976" (G. C. Bond, P. B. Wells, and F. C. Tompkins, Eds.). The Chemical Society, London.
22. Ekman, M. E., Anderegg, J. W., and Schrader, G. L., *J. Catal.* **117,** 246 (1989).
23. Konings, A. J. A., Valster, A., de Beer, V. H. J., and Prins, R., *J. Catal.* **76,** 466 (1982).